Materials Research Proceedings **32** (2023) 15-22 https://doi.org/10.21741/9781644902615-2

Achieving superplasticity in hard-to-deform metallic materials using high-pressure sliding (HPS) process

Zenji Horita[1,2,3,a*] and Yoichi Takizawa[4,b]

[1]School of Engineering, Kyushu Institute of Technology, Kitakyushu, 804-8550, Japan

[2]Synchrotron Light Application Center, Saga University, Saga, 840-8602, Japan

[3] Magnesium Research Center, Kumamoto University, Kumamoto 860-8555, Japan

[4]Technology Department, Nagano Forging Co., Ltd., Nagano 381-0003, Japan

[a]horita.zenji.688@m.kyushu-u.ac.jp, [b]ytakizawa@nsc-com.co.jp

Keywords: Severe Plastic Deformation, High-Pressure Sliding, Superplasticity, Superalloy, Cup Forming

Abstract. This presentation shows that superplasticity is achieved in hard-to-deform materials when they are processed by severe plastic deformation (SPD) through high-pressure sliding (HPS). The HPS process is similar to the high-pressure torsion (HPT) process as the straining is made under high pressure in highly constrained conditions. It is applicable to a sheet form of samples while the HPT process uses disks or rings, and thus it has advantage that the sample size can be increased. In addition, when the HPS process is combined with a feeding process, the SPD-processed area can be further enlarged without increasing the machine capacity, of which process is called the incremental feeding HPS (IF-HPS). The HPS process is applied to a Ni-based superalloy (Inconel 718), a Ti-6Al-7Nb alloy (F1295) and a Mg-6Al-1Zn alloy (AZ61), and superplasticity is well attained in all the hard-to-deform alloys with total elongations more than 400%. It is also demonstrated that cup forming of the Inconel 718 with practical dimensions is realized by application of the IF-HPS process.

Introduction

It is well established that the fine-grained structure is an important prerequisite for the advent of superplasticity. Severe plastic deformation (SPD) is a useful technique to produce such ultrafine-grained structures in many metallic materials [1]. In particular, SPD under high pressure such as using a process of high-pressure torsion (HPT) is of great importance because grain refinement is feasible even in hard-to-deform materials [2]. High-pressure sliding (HPS) [3,4] is also an SPD process under high pressure, and it is similar to the HPT process [5] as the straining is made under highly constrained conditions [6]. While the HPT process uses disks or rings and the sample size is rather limited, the HPS process is applicable to sheets and it has then advantage over the HPT process that the sample size can be increased as discussed in recent overview papers [7,8]. Furthermore, the HPS process provides a homogeneous development of microstructure throughout the sample [4]. However, the microstructure development is rather heterogeneous in the HPT-processed disk because the strain is introduced in proportion to the distance from the disk center so that it is more in the outer areas but is less in the inner area and theoretically zero at the center of the disk [6]. It should be noted that, when the HPS process is combined with a sample feeding process, the SPD-processed area can be further increased without increasing the machine capacity. This combined process, called the incremental feeding HPS (IF-HPS) [9], has been applied to hard-to-deform metallic materials such as a Ni-based superalloy (Inconel 718) [9,10] and a Ti-6Al-7Nb alloy (F1295) [10] including conventional Al alloys [11].

This presentation first gives a brief introduction of the HPS process and the IF-HPS process, and thus it is shown that superplastic elongation more than 400% is well attained in the former two

hard-to-deform alloys. It is also demonstrated that cup forming of the Inconel 718 with practical dimensions is realized by taking advantage of the superplasticiy through grain refinement by the IF-HPS process [9].

HPS

As illustrated in Fig. 1, sheet samples are placed between the anvils and the plunger. While applying a pressure on the anvils, the plunger was moved with respect to the anvils so that shear strain is introduced in the sample. Reciprocation of the plunger with respect to the anvils may be adopted to accumulate the strain [7,8]. It is noted that the HPS process is applicable not only to sheets [3,4] but also to rods [12] and pipes [13].

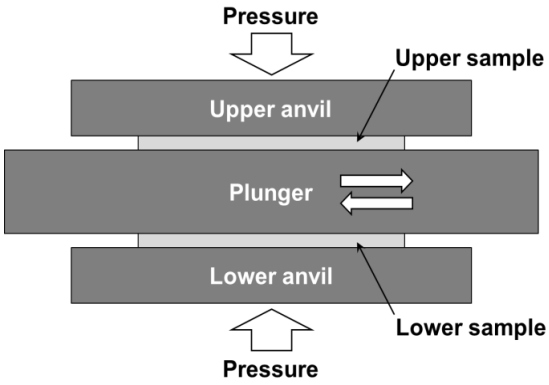

Fig. 1 *Schematic illustrations of high-pressure sliding (HPS).[7]*

IF-HPS

As illustrated in Fig.2, when a feeding process is incorporated in the HPS process, the SPD-processed area can be enlarged. This combined process, IF-HPS, has an advantage that upsizing is feasible without increasing the machine capacity. The conditions for optimal operation of the IF-HPS process was described in our recent overview paper [8] in terms of the following three points: (1) use of flat-type anvils to make sample feeding easier

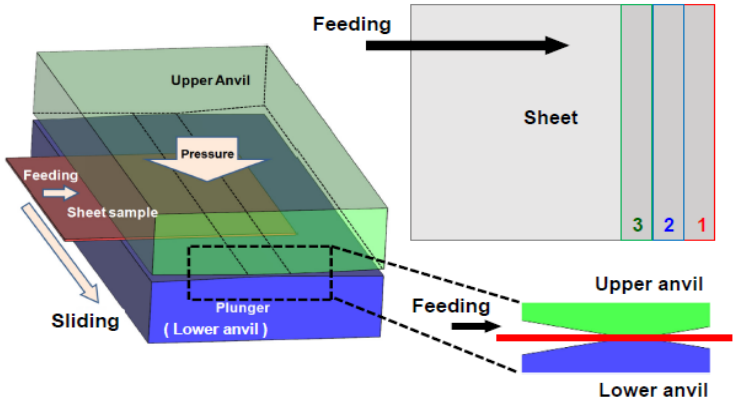

Fig. 2 *Schematic illustration of incremental feeding high-pressure sliding (IF-HPS).[9]*

and sheet surface smoother, (2) control of the sliding mode determined by the sliding distance and the numbers of the reciprocation of the sliding direction, and (3) control of the feeding pattern determined by the feeding distance and the feeding direction.

Application to Ni-based superalloy (Inconel 718)

Figure 3 shows a microstructure observed by a transmission electron microscope (TEM) after processing by HPS for a sliding distance of 15 mm under 4 GPa at room temperature [4]. It is

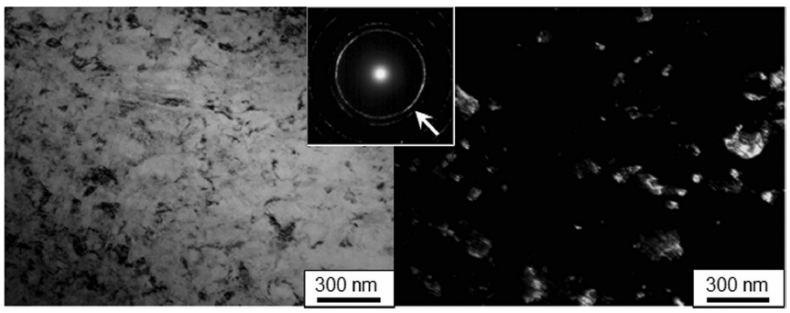

Fig.3 TEM bright-field image (left), dark-field image (right) and SAED pattern (center) for Inconel 718 alloy after processing by HPS for sliding distance of 15 mm under 4 GPa at room temperature.[4]

confirmed that the grain size is refined to ~100 nm from the dark-field image (on the right) taken by a diffracted beam indicated by the arrow in the selected area diffraction (SAED) pattern (at the center). Furthermore, the SAED pattern exhibits rings so that the structure consists of fine grains with high-angle boundaries. Nevertheless, the grain boundaries are ill-defined, and this is a typical feature observed in SPD-processed alloys [14].

Figure 4 shows results of tensile testing for HPS-processed specimens and those without processing, for comparison [15]. Here, the HPS-processing was made for an as-received state and an annealed state, while the underformed specimens include the as-received state, solution-treated state and solution-treated plus aged state. Tensile tests were conducted with an initial strain rate of 2×10^{-2} s^{-1} at 1073 K in all specimens for comparison. The unprocessed specimens were deformed only to 35% or less with maximum flow stresses exceeding 500 MPa, whereas supeplasticity was well attained to the total elongations more than 400% with the maximum flow stresses below 200 MPa in the HPS-processed specimens. It is clearly demonstrated that the HPS processing is effective to create a superplastic flow which gives rise to not only a significant reduction of the maximum flow stress but also to a significant increase in the total elongation.

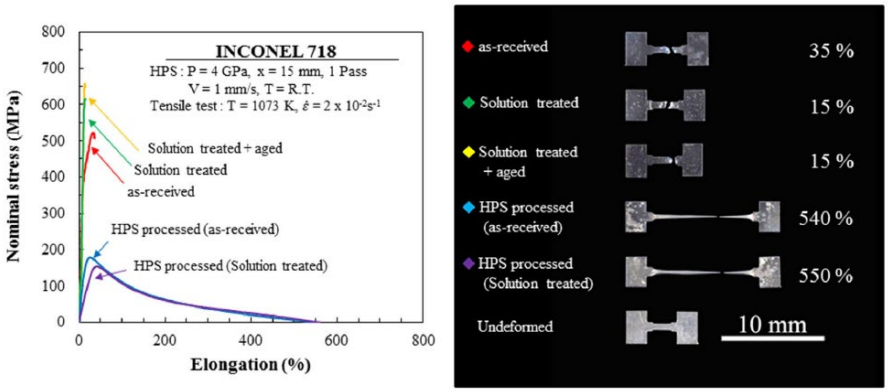

Fig.4. Stress-strain curves (left) and appearance of tensile specimens after deformation to failure (right) for as-received and solution-treated specimens with and without HPS processing including solution-treated plus aged specimen without HPS processing for comparison. All tensile specimens were deformed at 1073 K with initial strain rate of 2×10^{-2} s^{-1}.[15]

Tensile tests were further conducted at temperatures of 973, 1023, 1073, 1123 and 1173 K with initial strain rates in the range of 5.0×10^{-4} to 2×10^{-2} s^{-1} [15]. The total elongations are plotted against the initial strain rate in Fig.5. Here, the horizontal dotted line is drawn at the elongation of 400% above which is considered to be superplastic [16] and the vertical dotted line is drawn at the strain rate of 1x 10^{-2} s^{-1} beyond which the superplastic elongation is defined as the high-strain rate superplasiticity (HSRS) [17]. Inspection reveals that the HSRS was attained in the HPS-processed sample even though the temperature is as low as 1073 K, which is ~0.6 Tm where Tm is the melting temperature.

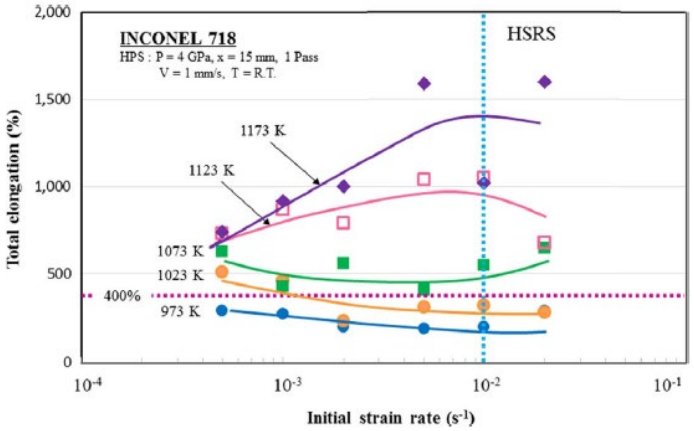

Fig. 5. Total elongation to failure plotted against initial strain rates for testing temperatures ranging from 973 K to 1173 K. Region of high strain rate superplasticity (HSRS) (> 400% and > 1×10^{-2} s^{-1}) is indicated by drawing horizontal and vertical dotted lines.[15]

The IF-HPS process was employed because the sample dimensions of 10 x 100 x 1 mm processed by a maximum capacity of the HPS machine is still insufficient. As shown in Fig.6, it was successful to cover a square area of a sheet with 100 x 100 mm without increasing the machine capacity [10]. Four tensile specimens were extracted from the sheet using an electrical discharge machine, where the traces of the extracted specimens are visible in the initial and ending sides as numbered 1 and 8, respectively. They were extracted from the shiny and rough surface areas. Here, the rough surface appeared because the anvil at the flat area was deliberately roughened to prevent slippage and the shiny surfaces arose because the sample was made contact with the smooth surfaces at both sides of the roughened parts of the anvil and plunger. All the tensile specimens exhibited superplastic elongations well more than 400% with maximum flow stresses reduced to ~ 200 MPa or less as shown in Fig.7.

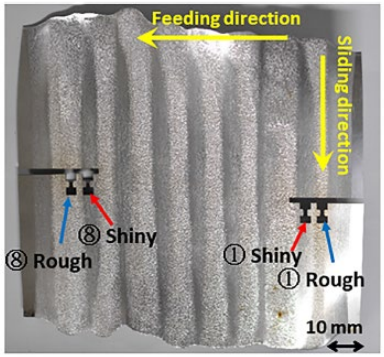

Fig. 6 Appearance of sheet sample after 8 passes of IF-HPS processing. [10]

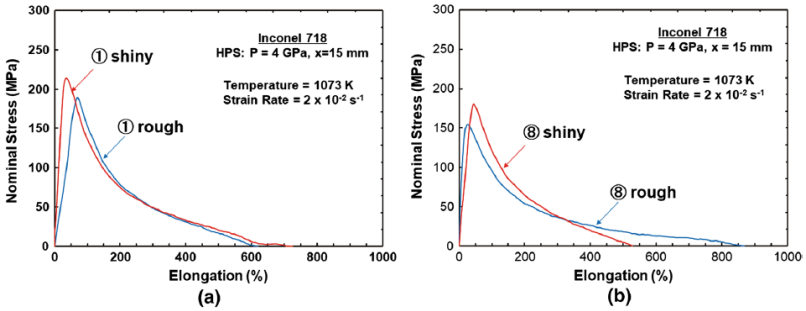

Fig. 7 Stress–strain curves at (a) initial and (b) ending sides of processed sheet. All tensile specimens were deformed at 1073 K with initial strain rate of 2 x 10^{-2} s^{-1}. [10]

Superplastic formability was further checked by extracting 30mm diameter disks from the IF-HPS processed sheet. The disk was then subjected to cup forming at 1073 K in air with a forming speed of 0.1mm/s. It was successful as shown in Fig. 8(a), whereas the disk without the IF-HPS processing was fractured at the flange as shown in Fig. 8(b) and many cracks appeared at the bottom of the cup even under the same forming condition.

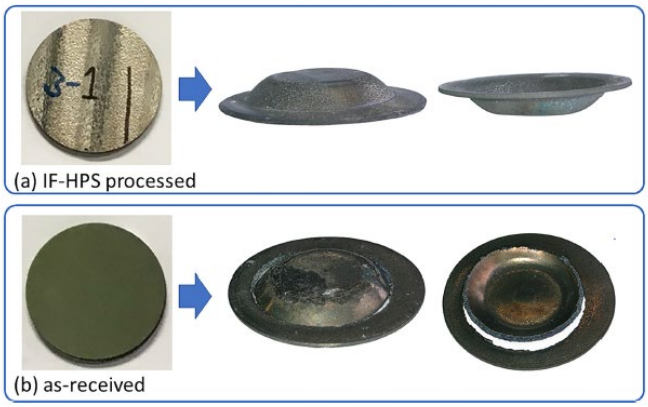

Fig. 8 Appearance of circular disks (left) extracted from IF-HPS processed sheet (upper) and as-received sheet (lower). Appearance after cup-shape forming (right) for IF-HPS-processed sheet (upper) and as-received sheet (lower). [8]

Figure 9 plots the total elongation to failure against the hardness measured on the Inconel 718 after processing by HPS including HPT from past studies [18]. There exists a linear relation, suggesting that it is possible to predict the advent of superplastic deformation by hardness measurement. Such a relation is reasonable because grain refinement promotes the total elongation at high temperatures due to enhanced contribution of grain boundary sliding to the total deformation [19]. The grain refinement can also enhance the room-temperature hardness due to the Hall-Petch strengthening mechanism [20,21].

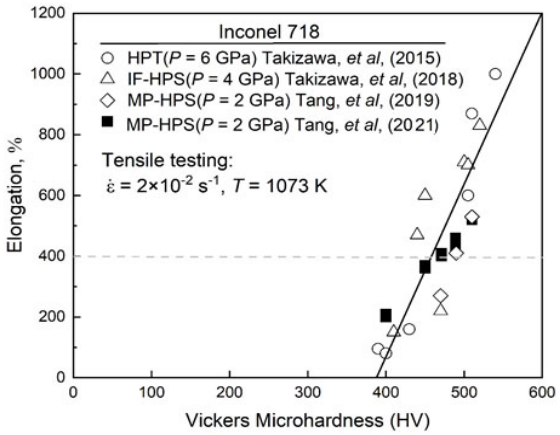

Fig. 9. Relation of total elongation plotted against hardness constructed using published data. Horizontal dotted line represents critical lower limit for superplasticity defined earlier [18].

Ti alloys

Figure 10 shows the stress-strain curves and the appearance of the tensile specimens of the F1295 alloy after processing through x = 10 mm under 3 GPa. The superplastic elongations more than 400% are confirmed. The tensile specimens are extracted from three different positions along the longitudinal axis of the sheet samples as shown in the inset. For comparison, the stress–strain curve and the appearance of a tensile specimen in the as-received state are included in Fig.10. While reduction in gage width is prominent in the as-received sample, more uniform deformation occurs throughout the gage length after the samples are processed by HPS.

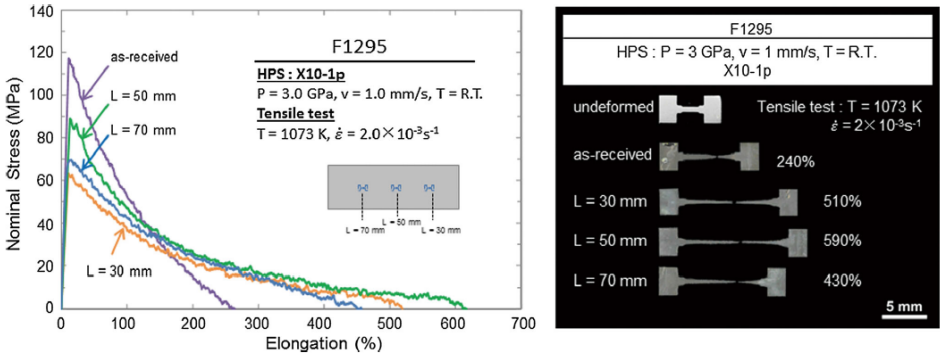

Fig. 10 Stress–strain curves (left) and appearance of tensile specimens after deformation to failure including undeformed specimen (right) for F1295 alloy. HPS was perfomed for sliding distance of 10 mm under 3 GPa at room

Mg alloys

Figure 11 shows the stress–strain curves and the appearance of the AZ61 samples processed for x = 10 mm at room temperature and at 403 K. The elongation to failure reached ~400% at both conditions with smooth and uniform elongations throughout the specimens. A close observation of microstructures after HPS processing at room temperature revealed that the grain size is refined to ~100 nm, but this fine-grained structure contains subgrains with low- angle boundaries. It is suggested that dynamic recrystallization should have occurred during the tensile testing because superplastic flow through grain boundary sliding hardly occurs in the subgrain structure but requires grain boundaries with high angles of misorientations.

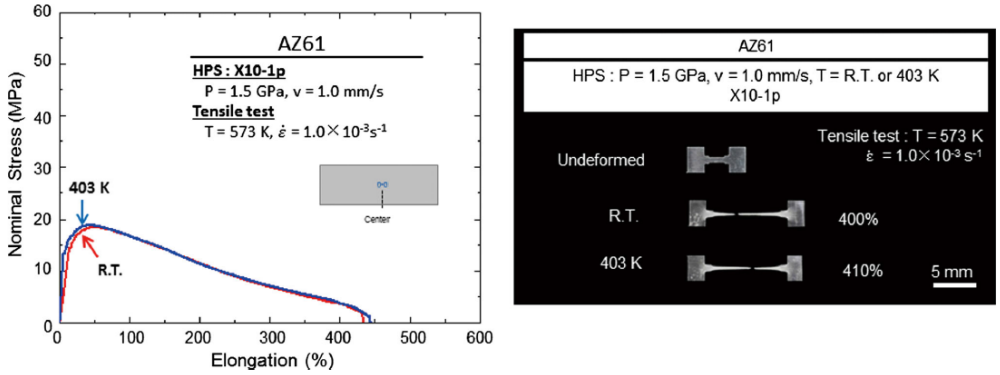

Fig. 11 Stress–strain curves (left) and appearance of tensile specimens after deformation to failure including undeformed specimen (right) for AZ61 alloy. HPS was performed for sliding distance of 10 mm under 1.5 GPa at room temperature and 403 K.

Summary and conclusions

Superplasticity successfully appeared in hard-to-deform metallic materials such as a Ni-based superalloy (Inconel 718), a Ti alloy (F1295) and a Mg alloy (AZ61) after processing by severe plastic deformation (SPD) though high-pressure sliding (HPS). In particular, high-strain rate superplasticity with a strain rate higher than $1x10^{-2}$ s^{-1} was attained in the Inconel 718 alloy. Incorporating a sample feeding process to the HPS process, called the incremental feeding HPS (IF-HPS), it was possible to enlarge the SPD-processed area as large as 100 x 100 mm in the Inconel 718 alloy without increasing the machine capacity. This enlargement thus enabled cup forming of the alloy without fracturing of the sample.

Acknowledgements
This study was conducted under a project subsidized by the New Energy and Industrial Technology Development Organization (NEDO).This study was also supported in part by a Grant-in-Aid for Scientific Research (A) from the MEXT, Japan (19H00830).

References

[1] R.Z. Valiev, Y. Estrin, Z. Horita, T.G. Langdon, M.J. Zehetbauer and Y.T. Zhu: JOM 58(4) (2006) 33-39. https://doi.org/10.1007/s11837-006-0213-7

[2] K. Edalati and Z. Horita: Mater. Sci. Eng. A 652 (2016) 325-352. https://doi.org/10.1016/j.msea.2015.11.074

[3] T. Fujioka and Z. Horita: Mater. Trans. 50 (2009) 930-933. https://doi.org/10.2320/matertrans.MRP2008445

[4] Y. Takizawa, T. Masuda, K. T. Fujimitsu, Kajita, K. Watanabe, M. Yumoto, Y. Otagiri and Z. Horita : Metall. Mater. Trans. A 47 (2016) 4669-4681. https://doi.org/10.1007/s11661-016-3623-3

[5] P.W. Bridgman: Phys. Rev. 48 (1935) 825-847. https://doi.org/10.1103/PhysRev.48.825

[6] A.P. Zhilyaev, T.G. Langdon: Prog. Mater. Sci. 53 (2008) 893-979. https://doi.org/10.1016/j.pmatsci.2008.03.002

[7] Z. Horita, Y. Tang, T. Masuda and Y. Takizawa : Mater. Trans. 61 (2020) 1177-1190. https://doi.org/10.2320/matertrans.MT-M2020074

[8] Y. Takizawa and Z. Horita: Mater. Trans. 64 (2023).https://doi.org/10.2320/matertrans.MT-MF2022025

[9] Y. Takizawa, K. Sumikazwa, K. Watanabe, T. Masuda, M. Yumoto, Y. Kanai, Y. Otagiri and Z. Horita : Metall. Mater. Trans. A 49 (2018) 1830-1840. https://doi.org/10.1007/s11661-018-4534-2

[10] Y. Takizawa, K.Watanabe, T. Kajita, K. Sumikawa, T. Masuda, M. Yumoto, Y. Otagiri and Z. Horita: J. Japan Inst. Met. Mater. 82 (2018) 25-31. https://doi.org/10.2320/jinstmet.J2017038

[11] T. Komatsu, T. Masuda, Y. Tang, I.F. Mohamed, M. Yumoto, Y. Takizawa and Z. Horita: Mater. Trans. 64 (2023) 436442. https://doi.org/10.2320/matertrans.MT-LA2022032

[12] T. Masuda, K. Fujimitsu, Y. Takizawa and Z. Horita: Lett. Mater. 5 (2015) 258263 https://doi.org/10.22226/2410-3535-2015-3-258-263

[13] Y. Tang, K. Matsuda, Y. Takizawa, M. Yumoto, Y. Otagiri and Z. Horita: Mater. Sci. Technol. 36 (2020) 877886. https://doi.org/10.1080/02670836.2020.1746538

[14] Z.Horita, D.J.Smith, M.Furukawa, M.Nemoto, R.Z.Valiev and T.G.Langdon: J. Mat. Res., 11 (1996) 1880-1890. https://doi.org/10.1557/JMR.1996.0239

[15] Y. Takizawa, T. Kajita, P. Kral, T. Masuda, K. Watanabe, M. Yumoto, Y. Otagiri, V. Sklenicka and Z. Horita: Mater. Sci. Eng. A 682 (2017) 603-612. https://doi.org/10.1016/j.msea.2016.11.081

[16] T.G. Langdon: J. Mater. Sci. 44 (2009) 5998-6010. https://doi.org/10.1007/s10853-009-3780-5

[17] K. Higashi, M. Mabuchi and T.G. Langdon: ISIJ Int. 36 (1996) 1423-1438. https://doi.org/10.2355/isijinternational.36.1423

[18] Y. Tang, K. Edalati, M. Masuda, Y. Takizawa, M. Yumoto, and Z. Horita: Mater. Lett. 300 (2021) 130144. https://doi.org/10.1016/j.matlet.2021.130144

[19] T.G. Langdon: Metall. Mater. Trans. A 13 (1982) 689-701. https://doi.org/10.1007/BF02642383

[20] E.O. Hall: Proc. Phys. Soc. B 64 (9) (1951) 747-753. https://doi.org/10.1088/0370-1301/64/9/303

[21] N.J. Petch: J. Iron. Steel Inst. 174 (1953) 25-28. https://doi.org/10.1111/j.1600-0447.1953.tb09440.x